ELSEVIER

www.elsevier.nl/locate/jorganchem

Journal of Organometallic Chemistry 609 (2000) 2–9

Journal of Organometallic Chemistry

Binding modes of a mixed donor multidentate iminobisphosphane ligand to the triosmium cluster: the crystal structures of $[\{Os_3(CO)_{11}\}_2(PNCHP)]$, $[Os_3(\mu\text{-}H)(\mu_3\text{-}PNCP)(CO)_7]$ and $[Os_3(\mu\text{-}H)(\mu_2\text{-}PNCP)(CO)_8]$

Eric W. Ainscough *[1], Andrew M. Brodie *[2], Anthony K. Burrell, Steven M.F. Kennedy

Department of Chemistry, Institute of Fundamental Sciences, Massey University, Private Bag 11-222, Palmerston North, New Zealand

Received 9 February 2000; received in revised form 23 May 2000

Abstract

The triosmium clusters $[Os_3(CO)_{11}(CH_3CN)]$ and $[Os_3(CO)_{10}(CH_3CN)_2]$ react with 2-(diphenylphosphino)-*N*-[2-(diphenylphosphino)benzylidene]benzeneamine (PNCHP) to give $[\{Os_3(CO)_{11}\}_2(PNCHP)]$ (**1**), two coordination isomers of $[Os_3(CO)_{11}(PNCHP)]$ (**2a**) and (**2b**), and 1,1-$[Os_3(CO)_{10}(PNCHP)]$ (**3**), respectively. When (**3**) is reacted with trimethylamineoxide the major product is $[Os_3(\mu\text{-}H)(CO)_7(\mu_3\text{-}PNCP)]$ (**4**) with two geometrical isomers of $[Os_3(\mu\text{-}H)(CO)_8(\mu_2\text{-}PNCP)]$ (**5a**) and (**5b**) being minor products. The clusters have been fully characterised by spectroscopic means and the structures of **1**·CH_2Cl_2, **4**·1.5CH_2Cl_2 and **5a** established by single-crystal X-ray analyses. In **1** PNCHP bridges two osmium triangles equatorially. In **4** the imine hydrogen of PNCHP has migrated to the osmium cluster and PNCP acts as a triply bridging nine electron donor, while in **5a** PNCP acts as a doubly bridging seven electron donor ligand.

Keywords: Osmium cluster; Crystal structure; Iminophosphane

1. Introduction

Doubly bridging ligands which donate more than six electrons to trinuclear clusters of ruthenium and osmium are uncommon and even fewer examples exist where the ligand is triply bridging [1]. The ligand in this report PNCHP or 2-$PPh_2(C_6H_4N{=}CHC_6H_4)$2-$PPh_2$, shown in Fig. 1, can be viewed as an extension of the ligand 2-$PPh_2(C_6H_4N{=}CHPh)$ which is found, minus the imino hydrogen, as a triply bridging seven electron donor in the complex $[Ru_3(\mu\text{-}H)(CO)_6(\mu_3\text{-}CPh{=}NC_6H_4PPh_2)(\mu\text{-dppm})]$ [2]. The ligand PNCHP has the potential to donate an additional two electrons to the cluster, making the ligand a rare example of a triply bridging nine electron donor. The only other example is found in the complex $[Os_3(\mu\text{-}H)(CO)_6(\mu_3\text{-}PPh_2CH_2P(Ph)C_6H_4CNR)(PPh_3)]$. However, in this case the ligand is not reacted directly with the triosmium cluster but formed from a subsequent C–C coupling reaction [3]. We report here, the reaction products of PNCHP with $[Os_3(CO)_{10}(CH_3CN)_2]$ followed by addition of trimethylamineoxide in situ in order to encourage the higher degrees of substitution desired. PNCHP was also reacted with $[Os_3(CO)_{11}(CH_3CN)]$ and $[Os_3(CO)_{10}(CH_3CN)_2]$ in the absence of trimethylamineoxide. In

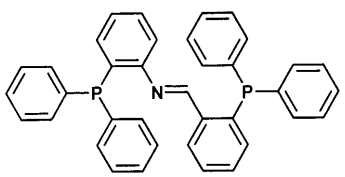

Fig. 1. The ligand 2-(diphenylphosphino)-*N*-[2-(diphenylphosphino)-benzylidene]benzeneamine (PNCHP).

[1] *Corresponding author. Fax: +64-6-3505682; email: e.ainscough@massey.ac.nz

[2] *Corresponding author.

0022-328X/00/$ - see front matter
PII: S0022-328X(00)00348-X

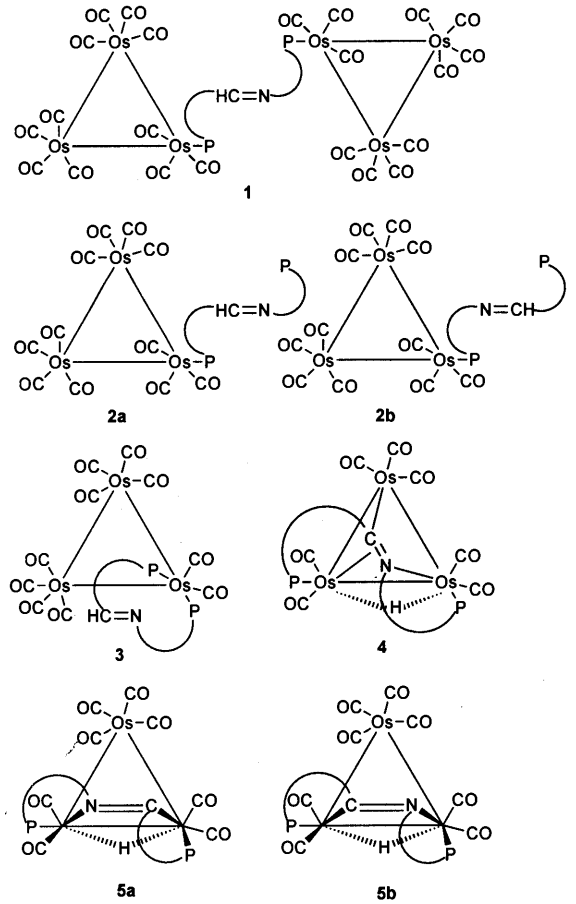

Fig. 2. The complexes showing the various coordination modes of PNCHP, where PNCHP is depicted by P–N=CH–P.

these cases the PNCHPs three inequivalent lone pairs of electrons, from the two phosphorus atoms and one nitrogen atom, are available to substitute for the acetonitrile ligand(s), hence, potential for several coordination isomers exist [4].

2. Results and discussion

2.1. Synthesis

The osmium cluster compounds described in this report are depicted schematically in Fig. 2. The PNCHP bridged dicluster species [{$Os_3(CO)_{11}$}$_2$-(PNCHP)] (**1**) was synthesised by reacting a half mole equivalent of the ligand PNCHP with [$Os_3(CO)_{11}$-(MeCN)]. The dimer is also obtained as a major product when attempting to synthesise the monomers, and coordination isomers of [$Os_3(CO)_{11}$(PHCNP)], (**2a**) and (**2b**) by reacting one mole equivalent of the ligand PNCHP with [$Os_3(CO)_{11}$(MeCN)]. The monomer **2a** was isolated by TLC, however, the monomer **2b** could not be separated from the dimer **1**. 1,1-[$Os_3(CO)_{10}$-(PNCHP)] (**3**) was synthesised by reacting the ligand PNCHP with [$Os_3(CO)_{10}(MeCN)_2$]. When **3** is reacted in situ with one or two equivalents of trimethylamineoxide, [$Os_3(\mu$-H)$(CO)_7(\mu_3$-PNCP)] (**4**) is obtained as the major product with two coordination isomers of [$Os_3(\mu$-H)$(CO)_8(\mu_2$-PNCP)] (**5a**) and (**5b**) as minor products. **5a** and **5b** are also observed in the ageing of **3**.

NMR and IR spectroscopic data for the complexes **1**–**5** are tabulated in Table 1 and mass spectral and microanalytical results are reported in the experimental section. FAB-mass spectral data for all the complexes recorded showed the expected molecular ion peaks with

Table 1
NMR and IR spectroscopic data for complexes **1**–**5**

Complex	^{1}H-NMR (ppm) [a]			^{31}P-NMR (ppm) [b]		ν(CO) (cm^{-1}) [c]			
	Os–H	CH=N	J(PH) (Hz)						
1		8.63		0.87	−1.8	2107m	2078w	2054s	2032s
						2019vs	1988m	1984sh	1952sh
2a		8.35		−1.9	−14.5	2108m	2057s	2033s	2020vs
						1989m	1980sh	1958sh	
2b		9.07d	6.4	−0.19	−15.3	[d]			
3		5.83 [e]		27.0	18.8	2093m	2056m	2034s	2009vs
						1995sh	1985s	1961sh	1940sh
4	−14.76dd		34.0, 5.7	33.4	14.6	2038vs	2009vs	1984m	1968m
						1952s	1935sh	1923sh	
5a/**b** [f]	−14.52dd		35.3, 4.5	32.9	26.3	2058s	1994vs	1967m	1960sh
	−14.97dd		41.4, 5.1	31.2	19.1	1937w	1927sh		

[a] Recorded at 270 MHz, chemical shifts are in ppm relative to $Si(CH_3)_4$, solvent $CDCl_3$.
[b] Recorded at 109 MHz, chemical shifts are in ppm relative to 85% H_3PO_4, solvent $CHCl_3$.
[c] In $CHCl_3$.
[d] Contaminated with **1**.
[e] Tentative assignment.
[f] A 1:1 mixture of two geometric isomers.

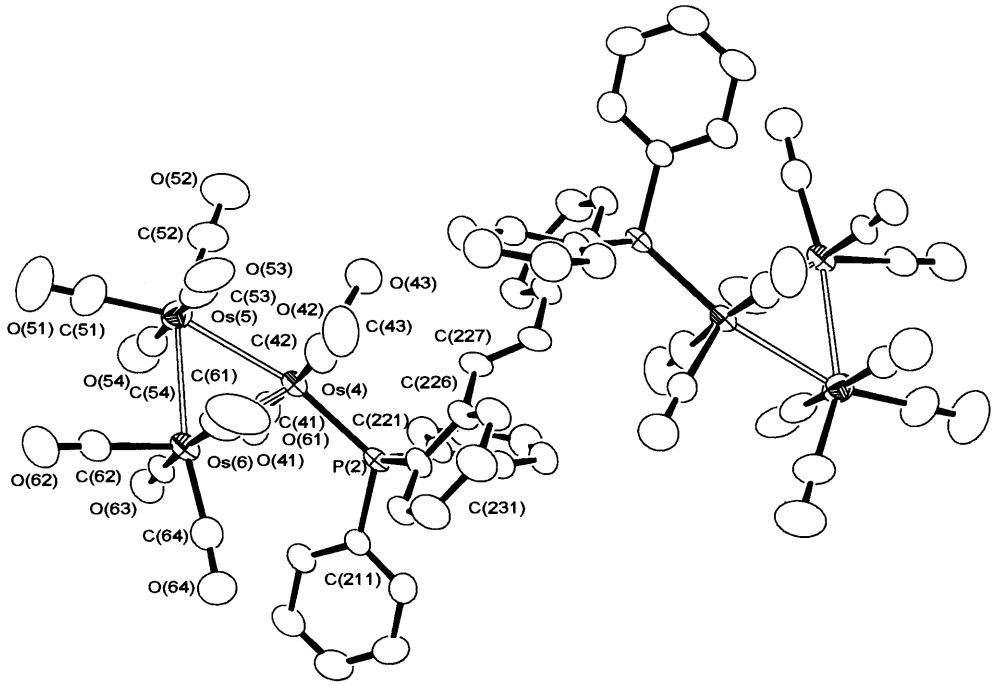

Fig. 3. ORTEP diagram for one molecule of $[\{Os_3(CO)_{11}\}_2(PNCHP)]$ (**1**) showing the numbering system used. Thermal ellipsoids are at the 50% probability level. Hydrogen atoms have been omitted for reasons of clarity.

the appropriate isotopic abundances and fragmentation patterns corresponding to the loss of successive carbonyl ligands.

Inspection of the infrared spectroscopic data shows a typical lowering of the carbonyl stretching energies from **1** through **5** consistent with the increasing degree of carbonyl substitution in the complex by the PNCHP ligand. **1** exhibited bands typical of $[Os_3(CO)_{11}]$ species [11,15] which is confirmed by its X-ray structure. Likewise for **2a** which gave a spectrum with no significant differences from **1**. Most $[M_3(CO)_{10}(L–L)]$ clusters, where M is Os or Ru and L–L is a bidentate ligand, tend to be found as 1,2-isomers [5]. However **3** was assigned the 1,1-isomer with equatorial bound phosphorus atoms, due to the similarity of its metal–carbonyl stretching region to other such species and dissimilarity to other isomers of $[Os_3(CO)_{10}L_2]$ [6–10,13,14].

Table 2
Selected bond lengths (Å) and angles (°) for $[\{Os_3(CO)_{11}\}_2(PNCHP)]$(**1**)·$CH_2Cl_2$ with estimated standard deviations in parentheses

Os(4)–Os(5)	2.8990(5)	Os(4)–P(2)	2.374(2)
Os(5)–Os(6)	2.8844(4)	Os–CO	1.881(9)–1.960(11)
Os(4)–Os(6)	2.9191(5)	C(227)–C(227′)	1.316(18)
P(2)–Os–CO_{eq}	99.2(3)	OC_{ax}–Os–CO_{eq}	87.7(4)–95.1(4)
OC_{eq}–Os–CO_{eq}	100.7(4)–102.7(5)		

2.2. Description of the crystal structures **1**·CH_2Cl_2, **4**·1.5CH_2Cl_2 and **5a**

2.2.1. Crystal structure of $[\{Os_3(CO)_{11}\}_2(PNCHP)]$(**1**)·$CH_2Cl_2$

X-ray analyses of **1** shows two independent molecules in the asymmetric unit. One of these is affected by disorder of the osmium triangle as discussed in Section 3. Both molecules in all other respects are essentially the same except for the symmetry generated imine bond lengths C(127)–C(127′) (1.266(17) Å) and C(227)–C(227′) (1.316(18) Å). It is unlikely that this difference is a real effect and probably arises from the crystallographically imposed symmetry which is present. One of the molecules is depicted in Fig. 3. The structure shows two '$Os_3(CO)_{11}$' moieties bridged by one PNCHP via the P atoms. The P atoms are coordinated in equatorial positions relative to the osmium triangle. A centre of inversion lies at the midpoint of the imine bond therefore it was not possible to distinguish the imino N from the imino C. Eleven carbonyl ligands occupy the remaining coordination sites to give a slightly distorted octahedral geometry for each osmium. Os–P, Os–CO and Os–Os bond lengths, listed in Table 2, are identical to those reported for $[Os_3(CO)_{11}(PPh_3)]$ [11] and similar to another reported iminophosphino-$Os_3(CO)_{11}$ species and the comparable complex $[\{Os_3(CO)_{11}\}_2(dppa)]$ (dppa is bis(diphenylphosphino)acetylene) [15,16].

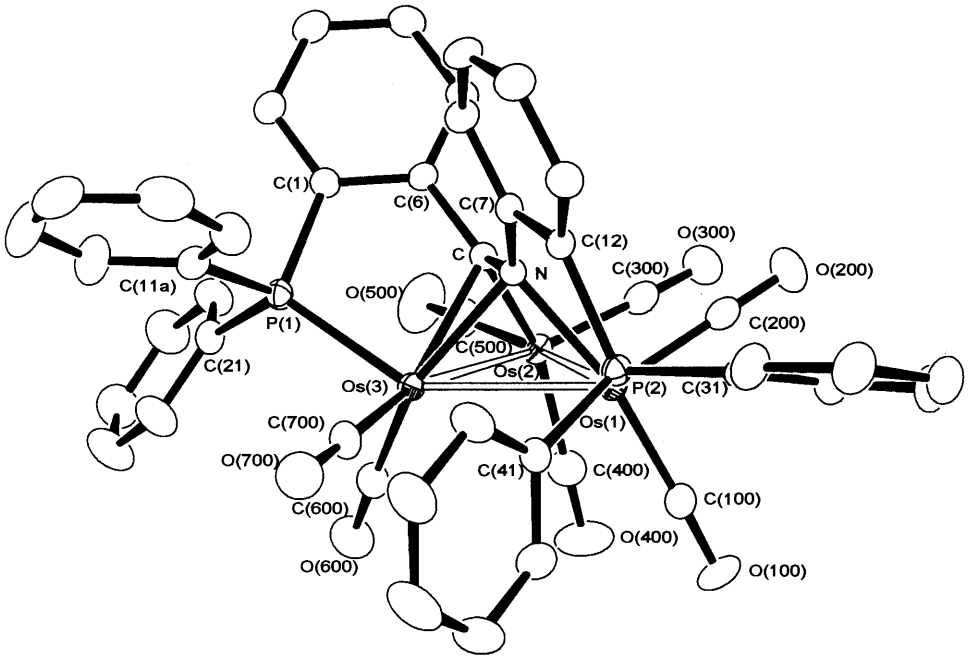

Fig. 4. ORTEP diagram for the complex $[Os_3(\mu\text{-}H)(\mu_3\text{-}PNCP)(CO)_7]$ (**4**) showing the numbering system used. Thermal ellipsoids are at the 50% probability level. Hydrogen atoms and solvent have been omitted for reasons of clarity.

2.2.2. Crystal structure of $[Os_3(\mu\text{-}H)(CO)_7(\mu_3PNCP)]$(4)·1.5$CH_2Cl_2$

Complex **4**, shown in Fig. 4, has at its centre an osmium triangle with the three Os–Os bond lengths at 2.7644(2) [Os(1)–Os(2)], 2.8523(2) [Os(1)–Os(3)] and 2.8290(2) Å (Os(2)–Os(3)), as listed in Table 3. An electron count of 48 electrons for the complex is supportive of three Os–Os bonds [12]. The imine bond N–C of the PNCP ligand caps the osmium triangle across its mid-point with the N atom lying directly above the Os(1)–Os(3) vector, relative to the plane of the osmium triangle, and the C atom likewise above the Os(2)–Os(3) vector. The imine-to-osmium triangle bonding distances are 2.130(3) [N–Os(1)], 2.210(3) [N–Os(2)], 2.050(4) [C(1)–Os(2)] and 2.253(4) Å [C–Os(3)]. The P atoms P(1) and P(2) are coordinated to Os(3) and Os(1), respectively in equatorial positions and have P–Os bond lengths of 2.3368(10) and 2.3326(10) Å which are typical for an osmium–arylphosphane bond [3,13–16]. Therefore the PNCP ligand is formally a nine-electron donor. To our knowledge only one other nine-electron donor ligand to Os or Ru has been reported [3,17]. The remaining coordination sites on the osmium triangle are filled by seven carbonyl ligands to give a distorted octahedral geometry around each Os atom. The Os–CO bond lengths ranged from 1.881(4)–1.933(5) Å. The imine bond N–C at a length of 1.414(5) Å has lengthened considerably relative to 1.296(8) Å found in the free-ligand [18]. However, this lengthening is expected as a result of the interaction of the imine bond with the osmium cluster [19–21]. In the PNCHP free-ligand the phosphane moieties are trans to the imine bond [18], however they are *cis* in **4**. The hydride that was observed by ^{1}H-NMR could not be located in the X-ray structure, but a cavity along the Os(1)–Os(3) edge, as determined by the angles C(600)–Os(3)–Os(1) (113.23(14)°), C(700)–Os(3)–Os(1) (108.68(13)) and C(100)–Os(1)–Os(3) (118.47(13)°), suggests a suitable position for H. In addition the longest Os–Os bond is at this edge which is consistent with a bridging H [22] and in the analogous system $[Ru_3(\mu\text{-}H)(CO)_6(\mu_3\text{-}CPh{=}NC_6H_4PPh_2)(\mu\text{-dppm})]$ [20] the H is proposed to bridge what would effectively be the Os(1)–Os(3) edge in **4**.

Table 3
Selected bond lengths (Å) and angles (°) for $[Os_3(\mu\text{-}H)(\mu_3\text{-}PNCP)(CO)_7]$(**4**)·1.5$CH_2Cl_2$ with estimated standard deviations in parentheses

Os(1)–Os(2)	2.7644(2)	Os(1)–N	2.130(3)
Os(1)–Os(3)	2.8523(2)	Os(2)–C	2.050(4)
Os(2)–Os(3)	2.8290(2)	Os(3)–N	2.210(3)
Os(3)–P(1)	2.3368(10)	Os(3)–C	2.253(4)
Os(1)–P(2)	2.3326(10)	Os–CO	1.881(4)–1.933(5)
		C–N	1.414(5)
N–Os(1)–P(2)	80.65(9)	P(2)–Os(1)–Os(3)	96.74(2)
C–Os(3)–P(1)	80.23(10)	P(1)–Os(3)–Os(1)	145.30(3)
Os(1)–N–Os(3)	82.16(11)	C(100)–Os(1)–Os(3)	118.47(13)
Os(2)–C–Os(3)	82.06(13)	C(600)–Os(3)–Os(1)	113.23(14)
		C(700)–Os(3)–Os(1)	108.68(13)

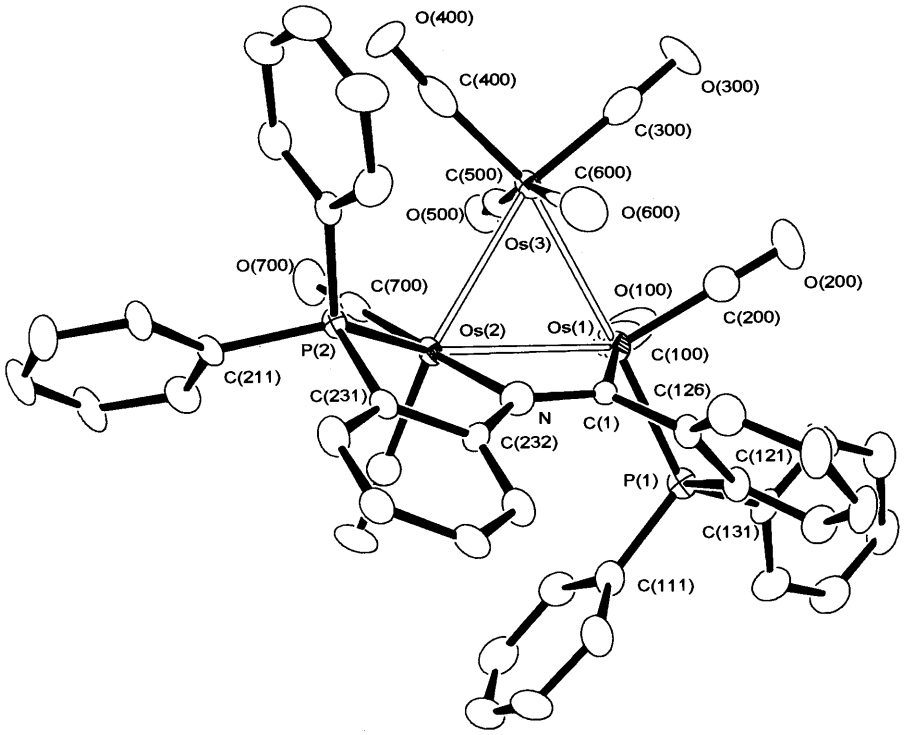

Fig. 5. ORTEP diagram for the complex $[Os_3(\mu\text{-H})(\mu_2\text{-PNCP})(CO)_8]$ (**5a**) showing the numbering system used. Thermal ellipsoids are at the 50% probability level. Hydrogen atoms have been omitted for reasons of clarity.

2.2.3. Crystal structure of $[Os_3(\mu\text{-H})(CO)_8(\mu_2\text{-PNCP})]$ (5a)

Complex **5a**, shown in Fig. 5 with selected bond lengths and angles listed in Table 4, can be viewed as a 'one carbonyl-group removal' step away from the previously discussed structure of **4**. Therefore the PNCP ligand binds to the osmium triangle in a similar fashion to **4** except that the distances 3.680(9) [N–Os(3)] and 3.610(9) Å [C(1)–Os(3)] are clearly non-bonding. In this case the PNCP ligand acts formally as a 7-electron donor. Again, the imine bond N–C(1) has lengthened relative to the free ligand (from 1.296(8) to 1.334(12)Å) but not to the extent found in **4** (1.414(5) Å), this is expected for a μ_2-imidoyl group compared with a μ_3-imidoyl group in terms of the electron density available for back-bonding into the antibonding orbital of the N=C bond [21]. The N and C(1) were unable to be distinguished from one another due to a half occupancy of each atom disordered over the two sites, hence a swapping of the N and C(1) labels of Fig. 5 gives the isomer **5b**. This was supported by the ^{1}H-NMR spectrum where two hydride signals are observed in a 1:1 ratio (Table 1). The hydride was not located but is proposed to be found bridging the Os(1)–Os(2) bond for the same reasons discussed for **4** above.

2.3. NMR spectroscopic studies

NMR spectroscopic data are given in Table 1. The hydride of $[Os_3(\mu\text{-H})(CO)_7(\mu_3\text{-PNCP})]$ (**4**) resonates at -14.76 ppm as a doublet of doublets. The coupling constants of 34.0 and 5.6 Hz have been assigned to ^2J(HP) hydride coupling to inequivalent P atoms. The hydride has been postulated, based on crystallographic evidence, to lie almost *trans* to one P atom and *cis* to the other as depicted in Fig. 2. Therefore the larger coupling constant has been assigned to the H involved in the *trans*-like H–Os–P angle and the smaller coupling constant to the H in the *cis* H–Os–P angle [19]. ^{31}P-NMR signals at 33.4(s) and 14.6(s) ppm support both phosphorus atoms being coordinated in solution [23].

$[Os_3(\mu\text{-H})(CO)_8(\mu_2\text{-PNCP})]$ exists as two isomers (Fig. 2 (**5a**) and (**5b**)) since it shows two hydride signals. They are at -14.52 and -14.97 ppm and both have a doublet of doublets splitting pattern with ^2J(HP) coupling constants of 35.3 and 4.5 Hz and 41.4 and 5.1 Hz, respectively. The integral ratio of the two hydride sig-

Table 4
Selected bond lengths (Å) and angles (°) for $[Os_3(\mu\text{-H})(\mu_2\text{-PNCP})(CO)_8]$ (**5a**) with estimated standard deviations in parentheses

Os(1)–Os(2)	2.9377(9)	Os(2)–N	2.130(8)
Os(1)–Os(3)	2.8565(8)	Os(1)–C(1)	2.130(9)
Os(2)–Os(3)	2.9218(7)	Os–CO	1.874(11)–1.940(11)
Os(1)–P(1)	2.322(3)	C(1)–N	1.334(12)
Os(2)–P(2)	2.320(2)		
N–Os(2)–P(2)	79.6(2)	P(1)–Os(1)–Os(2)	112.30(6)
C(1)–Os(1)–P(1)	74.1(2)	P(2)–Os(2)–Os(1)	140.36(6)

nals is 1:1 in the ^{1}H-NMR spectrum of the same crystals used for the crystallographic study. This ratio is reproducible. However, the ^{1}H-NMR spectrum recorded on a sample eluted from the chromatography band from which the crystals are grown (i.e. crude **5a**/**b**) show an integral ratio of 3:1 in favour of the signal at −14.97 and again this is reproducible. Therefore it is proposed that the product prefers to crystallise with the isomers in a 1:1 ratio. The ^{31}P-NMR of the crystals used for the X-ray diffraction study show four peaks, at 32.9(s), 31.2(s), 26.3(s) and 19.1(s) ppm. The peaks at 32.9 and 26.3 ppm have been tentatively assigned to one of the hydride isomers and the peaks at 31.2 and 19.1 ppm to the other hydride isomer. The closely related compound **4** has similar ^{31}P-NMR signals at 33.4 and 14.6 ppm.

The ^{1}H-NMR spectrum of [{$Os_3(CO)_{11}$}$_2$(PNCHP)] (**1**) exhibits a singlet resonance at 8.63 ppm compared with the free ligand value of 8.92(d) ppm which has been assigned to the imine proton. Other peaks present in the region 7.8–5.6 ppm were assigned to the 28 aromatic protons as confirmed by peak area integration. As expected, two singlets were observed in the ^{31}P-NMR spectrum at 0.87 and −1.8 ppm, both consistent with coordinated P atoms.

The coordination isomer **2a** displays an imine proton singlet at 8.35 while **2b** displays a doublet at 9.07 ppm. This phenomenon has been fully documented [18]. Both compounds show two peaks in their ^{31}P-NMR spectra, as shown in Table 1, consistent with one coordinated and one non-coordinated P atom. Although **2b** could not be separated from **1**, **2a** could be isolated pure. Subtraction of the NMR signals for pure **1** from that of the **1**/**2b** mixture enabled the assignments to be made for **2b**.

The ^{31}P-NMR signal shifts for **3** (Table 1), relative to the free PNCHP ligand, were consistent with the coordination of both P atoms to the osmium triangle. The ^{1}H-NMR signal at 5.83 ppm assigned to the imino-proton is at a considerably higher frequency than normally found for the coordinated ligand [4]. Unlike many osmium–carbonyl clusters, the ^{13}C-NMR spectrum of **3** showed the carbonyl ligands to be non-fluxional at room temperature and the cluster to have very low symmetry due to the complexity and number of ^{13}C resonances in the metal–carbonyl region of the spectrum.

3. Experimental

3.1. General methods

NMR measurements were performed on a JEOL GX270W spectrometer. IR spectra were recorded on a Perkin–Elmer FT-IR Paragon 1000 instrument. Mass spectra were obtained using a Varian VG70-250S double-focussing magnetic sector spectrometer by the LSIMS method using *m*-nitrobenzyl alcohol as the matrix. Isotope abundance simulations were performed to identify the parent ion. Microanalyses were performed by the Campbell Microanalytical Laboratory, University of Otago. Melting points were determined on a Bausch & Lomb hot plate melting point apparatus and are uncorrected with respect to calibration. [$Os_3(CO)_{11}(CH_3CN)$] and [$Os_3(CO)_{10}(CH_3CN)_2$] were prepared according to literature preparations. Solvents were dried by standard procedures. All reactions were carried out under an inert atmosphere.

3.2. Syntheses

3.2.1. [{$Os_3(CO)_{11}$}$_2$(PNCHP)] (1)

[$Os_3(CO)_{11}(CH_3CN)$] (0.251 g, 0.273 mmol) dissolved in dichloromethane (ca. 15 ml) and PNCHP (0.0749 g, 0.136 mmol) dissolved in the same solvent (ca. 3 ml) were combined and the mixture stirred at room temperature for 2.5 h. *n*-Hexane vapour was diffused into the reaction mixture to initiate crystallisation. The product, [{$Os_3(CO)_{11}$}$_2$(PNCHP)] (0.198 g, 63%) was isolated as large orange crystals, washed with *n*-pentane, and air-dried. M.p: 176°C (dec). (Found: C, 30.32; H, 0.96; N, 0.61; $C_{59}H_{29}NO_{22}Os_6P_2$ requires: C, 30.71; H, 1.27; N, 0.61). M^+ (^{192}Os) 2307.

3.2.2. [$Os_3(CO)_{11}$(PCHNP)] (2a)

[$Os_3(CO)_{11}(CH_3CN)$] (0.100 g, 0.109 mmol) dissolved in dichloromethane (ca. 10 ml) and PNCHP (0.0597 g, 0.109 mmol) in ca. 3 ml of the same solvent were combined and then heated under reflux for 30 min. The solvent was removed in vacuo giving yellow–orange microcrystals, which were purified by TLC, eluting with dichloromethane/*n*-hexane (2:1). Two major bands were obtained with R_f values of 0.91 and 0.53, respectively. The first band afforded a 5:1 mixture of [{$Os_3(CO)_{11}$}$_2$(PNCHP)] (**1**):[$Os_3(CO)_{11}$(PNCHP)] (**2b**)} (0.0384 g, 12%) as a yellow powder, the second band gave [$Os_3(CO)_{11}$(PNCHP)] (**2a**) (0.0252 g 16%) as a yellow powder, after isolation by filtration, washing with *n*-pentane and air-drying. M.p: 203°C (dec). MH^+ (^{192}Os) 1430.

3.2.3. 1,1-[$Os_3(CO)_{10}$(PNCHP)] (3)

[$Os_3(CO)_{10}(CH_3CN)_2$] (0.0955 g, 0.102 mmol) dissolved in dichloromethane (ca. 10 ml) and PNCHP (0.0562 g, 0.102 mmol) in ca. 3 ml of the same solvent were combined. The mixture was stirred at room temperature for 2 h. The solvent volume was reduced in vacuo and the reaction mixture purified by TLC, eluting with 3:1 dichloromethane–*n*-hexane. The major band was extracted into dichloromethane and the product precipitated with hexamethyldisiloxane as an

Table 5
Crystallographic data for [{$Os_3(CO)_{11}$}$_2$(PNCHP)](**1**)·CH_2Cl_2, [Os_3(μ-H)(μ$_3$-PNCP)$(CO)_7$](**4**)·1.5CH_2Cl_2 and [Os_3(μ-H)(μ$_2$-PNCP)$(CO)_8$] (**5a**/**b**)

Compound	**1**·CH_2Cl_2	**4**·1.5CH_2Cl_2	**5a**/**b**
Empirical formula	$C_{60.51}H_{32}Cl_3O_{20.50}Os_6P_2$	$C_{45}H_{30}Cl_2NO_7Os_3P_2$	$C_{45}H_{29}NO_8Os_3P_2$
Formula weight	2396.49	1400.14	1344.23
Temperature (K)	203(2)	200(2)	171(2)
Wavelength (Å)	0.71073	0.71073	0.71073
Crystal system	Triclinic	Triclinic	Triclinic
Space group	$P\bar{1}$	$P\bar{1}$	$P\bar{1}$
Unit cell dimensions			
a (Å)	11.14790(10)	11.50110(10)	11.289(3)
b (Å)	17.003(2)	11.7702(2)	11.709(3)
c (Å)	19.5194(2)	17.2844(2)	17.143(5)
α (°)	105.3140(10)	70.5570(10)	84.433(3)
β (°)	104.9670(10)	86.44(1)	77.697(3)
γ (°)	98.2070(10)	78.6220(10)	70.918(4)
Volume (Å^3)	3358.00(5)	2162.98(5)	2091.3(9)
Z	2	2	2
D_{calc} (Mg m^{-3})	2.370	2.150	2.135
Absorption coefficient (mm^{-1})	11.545	9.039	9.223
Crystal size (mm^3)	0.56 × 0.30 × 0.18	0.40 × 0.36 × 0.28	0.68 × 0.48 × 0.30
Theta range for data collection (°)	1.14–27.46	1.25–27.46°.	1.95–26.42
Index ranges	$-13 \le h \le 14$, $-21 \le k \le 21$, $-25 \le l \le 24$	$-14 \le h \le 14$, $-15 \le k \le 15$, $-22 \le l \le 22$	$-13 \le h \le 14$, $-14 \le k \le 14$, $-21 \le l \le 21$
Reflections collected	31 036	21 157	26 697
Independent reflections	14 322 [$R_{int} = 0.0533$]	9351 [$R_{int} = 0.0195$]	8407 [$R_{int} = 0.0664$]
Absorption correction	Semi-empirical from equivalents	Semi-empirical from equivalents	Semi-empirical from equivalents
Max. and min. transmission	0.2304 and 0.0596	0.1863 and 0.1227	0.1684 and 0.0619
Completeness of data in 2θ	100%	100%	100%
Refinement method	Full-matrix least-squares on F^2	Full-matrix least-squares on F^2	Full-matrix least-squares on F^2
Data/restraints/parameters	14322/976/906	9351/0/536	8407/0/517
Goodness-of-fit on F^2	0.930	1.153	1.003
Final R indices [$I > 2\sigma(I)$] [a]	$R_1 = 0.0478$, $wR_2 = 0.1289$	$R_1 = 0.0230$, $wR_2 = 0.0584$	$R_1 = 0.0428$, $wR_2 = 0.1010$
R indices (all data)	$R_1 = 0.0667$, $wR_2 = 0.1473$	$R_1 = 0.0261$, $wR_2 = 0.0607$	$R_1 = 0.0640$, $wR_2 = 0.1102$
Hydrogen treatment	Mixed	Mixed	Mixed
Largest differrence peak and hole (e Å^{-3})	2.954 and −3.044	1.185 and −1.424	3.201 and −3.955

[a] $wR_2 = [\Sigma[w(F_o^2 - F_c^2)^2]/\Sigma[w(F_o^2)^2]]^{1/2}$ where $w^{-1} = [\sigma^2(F_o^2) + (aP)^2 + bP]$ for **5a** ($a = 0.061$; $b = 0.0$), **4**·1.5CH_2Cl_2 ($a = 0.10$; $b = 0.0$), and **1**·CH_2Cl_2 ($a = 0.0267$; $b = 4.2293$) $P = [\max(F_o^2, 0) + 2F_c^2]/3$. The structures were refined of F_o^2 using all data; $R_1 = \Sigma||F_o| - |F_c||/\Sigma|F_o|$.

orange powder, washed with *n*-pentane, and air-dried to give 1,1-[$Os(CO)_{10}$(PNCHP)] (0.0280 g, 27%). The compound is very soluble in all common solvents. Found: C, 37.48; H, 2.19; N, 0.89. $C_{49}H_{31}Cl_2NO_{10}OsP_2$ requires: C, 37.44; H, 2.29; N, 1.04). $[M–H]^+$ (^{192}Os) 1400. ^{13}C-NMR δ *C*O ($CDCl_3$): 193.22(d), 5.49; 193.18(s); 190.46(d) 7.32; 190.16(s); 188.59(d), 6.72; 186.72(d), 6.71 Hz; 179.68(d), 3.67; 178.49(d), 2.44; 172.67(d), 2.44 Hz; 170.32(s).

3.2.4. [Os_3(μ-H)$(CO)_7$(μ$_3$-PNCP)] (**4**)

[$Os_3(CO)_{10}(CH_3CN)_2$] (0.0960 g, 0.103 mmol) and PNCHP (0.0561 g, 0.102 mmol) were combined in dichloromethane (45 ml) and stirred at room temperature for 110 min, to form 1,1-[$Os_3(CO)_{10}$(PNCHP)] in situ. Freshly sublimed trimethylamineoxide (0.0155 g, 0.206 mmol) in acetonitrile (ca. 5 ml) was added dropwise to the red–orange solution over 135 min. The reaction mixture was stirred for a further 22 h then taken to dryness in vacuo. The product was crystallised from dichloromethane/*n*-hexane by vapour diffusion to give the product as large orange crystals (0.0404 g, 30%). M.p: 182°C (dec). Found: C, 38.82; H, 2.13; N, 1.15. $C_{45}H_{31}Cl_2NO_7Os_3P_2$ requires: C, 38.66; H, 2.19; N, 0.98). M^+ (^{192}Os) 1317.

3.2.5. [Os_3(μ-H)$(CO)_8$(μ$_2$-PNCP)] (**5a**/**b**)

[$Os_3(CO)_{10}(CH_3CN)_2$] (0.0910 g, 0.0976 mmol) and PNCHP (0.0538 g, 0.0979 mmol) were combined in dichloromethane (ca. 12 ml) and heated to reflux for 30 min. Freshly sublimed trimethylamineoxide (0.0147 g, 0.196 mmol) in dichloromethane (ca. 5 ml) was added dropwise to the red reaction mixture, resulting in a colour change to very dark-brown after 1 h. After a further 1 h when the reaction mixture became red again, it was allowed to cool. It was passed through a small alumina column (200–400 mesh) to remove any excess trimethylamineoxide, eluting with dichloro-

methane. The solvent was then removed in vacuo. The crude reaction product(s) was run down a silica gel (100–200 mesh) column, eluting successively with 0, 1, 10, and 100% solutions of methanol in dichloromethane, to give an orange, yellow, yellow and yellow band, respectively. The fractions were taken to dryness in vacuo. The major band was the first orange band and this was further purified by TLC, eluting with dichloromethane. The product was crystallised from dichloromethane–*n*-hexane by vapour diffusion to give the product as red–orange crystals (0.0014 g, 1%). Microanalytical data could not be obtained due to insufficient amount of sample. M^+ (^{192}Os) 1345. This compound is also observed in the ageing of **3** and in the synthesis of **4**.

3.3. Molecular structure determination of $[\{Os_3(CO)_{11}\}_2(PNCHP)]$(**1**)$\cdot CH_2Cl_2$, $[Os_3(\mu\text{-}H)(CO)_7(\mu_3\text{-}PNCP)]$(**4**)$\cdot 1.5CH_2Cl_2$ and $[Os_3(\mu\text{-}H)(CO)_8(\mu_2\text{-}PNCP)]$ (**5a**)

Data collection and refinement were performed as previously described using a Siemens SMART diffractometer Mo–K_α radiation, graphite monochromator, $\lambda = 0.71073$ Å [24]. The relevant details are given in Table 5. Refinements for **4**$\cdot 1.5CH_2Cl_2$ and **5a** were routine. However, **1**$\cdot CH_2Cl_2$ contains a significant disorder. There are two independent molecules which are generated by the symmetry operation. As a result of the symmetry operation the imine nitrogen and carbon are disordered and were modelled using carbon atoms. Furthermore, one of the independent molecules has two different orientations for the Os triangle. The disorder was modelled using 86% occupancy for the major component [Os(**1a**), Os(**2a**), Os(**3a**)] and 14% for the minor [Os(**1b**), Os(**2b**), Os(**3b**)]. Unfortunately, it was not possible to identify the carbonyl ligands from difference maps for the minor occupancy Os triangle and these have been omitted from the refinement.

4. Supplementary data

Crystallographic data for the structural analysis has been deposited with the Cambridge Crystallographic Data Centre, CCDC no. 139389 for compound **1**, 139390 for compound **4** and 139391 for compound **5a**. Copies of this information may be obtained free of charge from: The Director, CCDC, 12 Union Road, Cambridge, CB2 1EZ, UK (Fax: +44-1223-336033; e-mail: deposit@ccdc.cam.ac.uk or www: http://www.ccdc.cam.ac.uk).

Acknowledgements

We thank the Massey University Research Fund for financial support.

References

[1] E.W. Abel, F. Gordon, A. Stone, G. Wilkinson (Eds.), Comprehensive Organometallic Chemistry II: A Review of the Literature 1982–1984, Pergamon, Oxford, 1995, pp. 700–709 (and references within).
[2] C.J. Adams, M.I. Bruce, O. Kühl, B.W. Skelton, A.H. White, J. Organomet. Chem. 445 (1993) C6.
[3] K.L. Lu, H.J. Chen, P.Y. Lu, S.Y. Li, F.E. Hong, S.M. Peng, G.H. Lee, Organometallics 13 (1994) 585.
[4] E.W. Ainscough, A.M. Brodie, A.K. Burrell, S.M.F. Kennedy, J.M. Waters, P.D. Buckley, J. Chem. Soc. Dalton Trans. (accepted for publication).
[5] E.W. Abel, F. Gordon, A. Stone, G. Wilkinson (Eds.), Comprehensive Organometallic Chemistry II: A Review of the Literature 1982–1984, Pergamon, Oxford, 1995, p. 715 (and references within).
[6] A.J. Deeming, S. Donovan-Mtunzi, S.E. Kabir, J. Organomet. Chem. 333 (1987) 253.
[7] G. Süss-Fink, H. Jungbluth, J. Organomet. Chem. 352 (1988) 185.
[8] A.J Deeming, S. Donovan-Mtunzi, S.E. Kabir, P.J. Manning, J. Chem. Soc. Dalton Trans. (1985) 1037.
[9] A.J. Deeming, M.B. Smith, J. Chem. Soc. Chem. Commun. (1993) 844.
[10] D. Heijdenrijk, J.T.B.H. Jastrzebski, G. van Koten, T. Mahabiersing, C.H. Stam, K. Vrieze, R. Zoet, Organometallics 7 (1988) 2108.
[11] M.I. Bruce, C.A. Hughes, M.J. Liddell, B.W. Skelton, A.H. White, J. Organomet. Chem. 347 (1988) 157.
[12] E.W. Abel, F. Gordon, A. Stone, G. Wilkinson (Eds.), Comprehensive Organometallic Chemistry II: A Review of the Literature 1982–1984, Pergamon, Oxford, 1995, p. 689 (and references within).
[13] D. Braga, F. Grepioni, C. Gradella, B.F.G. Johnson, J. Lewis, M. Monari, J. Chem. Soc. Dalton Trans. (1990) 2863.
[14] A.J. Deeming, S. Donovan-Mtunzi, K.I. Hardcastle, K. Henrick, S.E. Kabir, M. McPartlin, J. Chem. Soc. Dalton Trans. (1988) 579.
[15] C.J Adams, P. Braunstein, M.I. Bruce, S.C. Cea, W.R. Cullen, P.A. Duckworth, P.A. Humphrey, O. Kühl, B.W. Skelton, E.R.T. Tiekink, A.H. White, J. Organomet. Chem. 467 (1994) 251.
[16] A.J. Amoroso, B.F.G. Johnson, J. Lewis, A.D. Massey, P.R. Raithby, W.T. Wong, J. Organomet. Chem. 440 (1992) 219.
[17] E.W. Abel, F. Gordon, A. Stone, G. Wilkinson (Eds.), Comprehensive Organometallic Chemistry II: A Review of the Literature 1982–1984, Pergamon, Oxford, 1995, p. 709 (and references within).
[18] X. Fan, MPhil Thesis, Massey University, New Zealand, 1995.
[19] M. Day, D. Espitia, K.I. Hardcastle, S.E. Kabir, E. Rosenberg, Organometallics 10 (1991) 3550.
[20] C.J. Adams, M.I. Bruce, O. Kühl, B.W. Skelton, A.H. White, J. Organomet. Chem. 445 (1993) C6.
[21] R.D. Adams, N.M. Golembeski, Inorg. Chem. 17 (1978) 1969.
[22] E.W. Abel, F. Gordon, A. Stone, G. Wilkinson (Eds.), Comprehensive Organometallic Chemistry II: A Review of the Literature 1982–1984, Pergamon, Oxford, 1995, p. 715 (and references within).
[23] S. Berger, S. Braum, H.-O. Kalinowski, NMR Spectroscopy of the Non-metallic Elements, Wiley, Chichester, 1997, p. 835.
[24] A.K. Burrell, K.C. Gordon, S.E. Page, Inorg. Chem. 37 (1998) 4452.